Appl Biochem Biotechnol
DOI 10.1007/s12010-014-0988-x

Template-Assisted Electrochemical Growth of Polypyrrole Nanotubes for Development of High Sensitivity Glucose Biosensor

Pragya Agar Palod · Shyam S. Pandey · Shuji Hayase · Vipul Singh

Received: 28 January 2014 / Accepted: 19 May 2014

Abstract In this paper, we report the growth of polypyrrole (PPy) nanotube arrays using template-assisted electrochemical polymerization to fabricate enzymatic glucose biosensors. The PPy nanotubes were grown on platinum-coated alumina membranes (Anodisc™s). By varying the polymerization time during the potentiostatic electropolymerization, the size/diameter of the PPy nanotubes were controlled, leading to changes in the subsequent enzyme immobilization (via physical adsorption). Enzyme electrode thus fabricated resulted in to the optimum sensitivity of 18.6 mA cm^{-2} M^{-1}, a wide range of linear operation (0.25–20 mM) and the lowest detection limit of 0.25 mM glucose concentration for the biosensor with the polymerization time of 40 s. The effect of polymerization duration on the sensitivity has been explained on the basis of porosity and enzyme-loading capacity of polymerized electrodes.

Keywords Glucose biosensor · Polypyrrole · Glucose oxidase · Amperometric · Sensitivity · Porosity · Anodisc™

Introduction

Sugars constitute a class of biocomponents, which plays a very important role in human metabolism. Among them, glucose is a key analyte in fields ranging from food industry to biomedical analysis [1]. Although many analytical techniques have been reported based on reduction of glucose, viz., colorimetric methods, etc. However, owing to their poor selectivity, the usage of these methods mandates prior purification of proteins making the analysis laborious and time consuming [2]. Biosensors have emerged as a viable alternative to the

P. A. Palod · V. Singh (✉)
Molecular and Nanoelectronics Research Group (MNRG), Department of Electrical Engineering, Indian Institute of Technology Indore, Pithampur Auto Cluster Limited (PACL) Building, Survey No. 113/2-B, Village Hernia Khedi, Mhow, Indore, Madhya Pradesh, India
e-mail: vipul.iiti@gmail.com

S. S. Pandey · S. Hayase
Department of Biological Functions and Engineering, Graduate School of Life Science and Systems Engineering, Kyushu Institute of Technology, 2-4 Hibikino, Wakamatsu, Kitakyushu-shi, Fukuoka, Japan

Published online: 10 June 2014

existing conventional techniques. The research in this field has been accelerated in the past few decades for various applications such as glucose monitoring, drug discovery, drug analysis, food analysis, etc. Of these, more than 85 % of biosensor market is captured by glucose biosensors due to tremendous increase in number of diabetic patients worldwide [3]. Glucose concentration in human body is controlled by insulin, as it absorbs the blood glucose and converts it into energy. In a healthy person, glucose concentration typically ranges between 80 and 120 mg dL^{-1} (4.4–6.6 mM).

Biosensors are sophisticated analytical instruments which incorporate a bio recognition element (e.g., enzyme, nucleic acid, antibody, whole cell) in close contact to a transducer. The latter senses the changes that take place in the system, as a result of the substrate (analyte)-biocatalyst (enzyme) interaction [4]. The transduced parameter can be electrical, optical, thermal, or piezoelectric. Among these biosensors, enzyme electrodes combine the specificity and selectivity imparted by the biomolecule, to the accuracy, sensitivity, and rapidity of the physicochemical transduction and necessitates minimum sample treatment. Biosensors based on enzyme immobilization provide the advantages of repetitive enzyme use, biocatalyst stabilization, cost reduction, etc. Some of the already reported techniques for enzyme immobilization are physical adsorption, gel entrapment, covalent coupling with or without cross-linking, or the construction of chemically modified electrodes based on carbon paste, carbon nanotubes, composite materials, screen printing, or sol-gel technique [5, 6].

Conducting polymers (CPs) owing to their ability to be doped, electronic conductivity, and biocompatibility are being intensively investigated as active or functional materials in various electronic as well as electrochemical biosensors [5, 7]. In this context, polypyrrole (PPy) is one of the most significant CPs because of its high electronic conductivity, high environmental stability, and inherent biocompatibility [8, 9]. In the past decade, the role of PPy as a supporting matrix for enzyme immobilization in various enzymatic biosensors has been extensively studied by researchers worldwide [8, 10]. Though CPs can be synthesized using various chemical as well as electrochemical methods, electrochemical synthesis is one of the most preferred methods for obtaining PPy thin films on a conductive substrate because of the good solubility of pyrrole monomer in a wide range of aqueous as well as non-aqueous solvents and its low oxidation potential for electrooxidation [10–13]. CP-based nanostructures have been reported to have much higher electrochemical activity than their bulk counterparts due to their higher specific surface area [13, 14]. Hence, enhanced interaction between CP and analyte leads to improved response and sensitivity of biosensors [14, 15].

With the aim of achieving high quality biosensors with high accuracy, high sensitivity, wide operational range, relatively longer shelf life, etc., several variations in terms of supporting matrix material, growth method, and immobilization techniques are currently being utilized. Ekanayake et al. have studied the effect of immobilization techniques on the biosensor performance [16]. Raicopol et al. utilized PPy-carbon nanotube (CNT) composite with glucose oxidase (GO_x) immobilization using entrapment [17]. Physical adsorption, being the simplest and easiest of all immobilization methods, has attracted most of the researchers. As immobilization by this method involves only electrostatic interactions and no chemical reactions; hence, the possibility of enzyme denaturation due to conformational changes is minimized [6].

Two types of methods, viz., template-based and template-free synthesis of CP nanostructures, have been reported in literature, each having its own merits [14, 18, 19]. Template-based method was pioneered by Martin et al. and has received considerable attention over the years due to its simplicity, controllability, and widespread applications [20, 21]. Some of the frequently used hard templates are zeolites, track-etched polymeric membranes, anodically oxidized alumina membranes (Anodisc™), etc. [21]. In this paper, we report template-assisted

electrochemical polymerization of PPy nanostructures on a confined path dictated by the walls of cylindrical pores of alumina Anodisc™. The synthesis of nanotube or nanowire arrays along the porous walls of the Anodisc™ is highly dependent on the experimental parameters such as applied potential or current density, monomer and supporting electrolyte concentrations, polymerization duration, etc. Xiao et al. studied growth of various conducting polymers using porous alumina templates and concluded that low monomer concentration and high polymerization potential are required for growth of polymer nanotubes [22].

In this work, PPy nanotube arrays were synthesized by potentiostatic electrochemical oxidation of pyrrole monomer on the platinum-coated Anodisc™ each having a pore diameter of 200 nm. The polymerized electrodes were used as a supporting matrix for GO_x immobilization. The glucose-biosensing response was examined using amperometric detection technique. As improvements in sensitivity of biosensors have always been of interest, polymerization time was optimized for the best sensitivity.

Experimental

1. Reagents

All required chemicals including pyrrole monomer, hydrogen peroxide (H_2O_2) lithium perchlorate ($LiClO_4$), sodium phosphate dibasic (Na_2HPO_4), sodium phosphate monobasic (NaH_2PO_4), D-(+)-glucose, uric acid, L-ascorbic acid, and glucose oxidase from *Aspergillus niger* (E. C. 1.1.3.4) were used as obtained from Sigma-Aldrich. All the chemicals were of analytical grade. Anodisc™s (pore diameter 200 nm) were purchased from Whatman. Deionized water (DI) of 18 MΩ resistivity was used for preparation of aqueous solutions. A 50-mM phosphate buffer solution (PBS) of pH 6.8 was prepared using NaH_2PO_4, Na_2HPO_4, and deionized (DI) water.

2. Electrochemical cell

All electrochemical experiments including activity assay, electropolymerization, and response current measurements were performed at room temperature in a three-electrode electrochemical cell using electrochemical station (Autolab PGSTAT302N). Platinum foil and Ag/AgCl were used as counter and reference electrodes, respectively.

3. Fabrication and characterization of electrodes

Figure 1 presents the schematic illustration of cross-sectional view of fabricated PPy/Pt/Anodisc™ electrode. Patterned Pt electrode (defined by mask) was coated on the Anodisc™ using direct current magnetron-sputtering system operated at base pressure of 2×10^{-7} mbar. During deposition, argon gas flow rate was maintained at 20 cm^3 min^{-1}. Deposition rate and pressure during sputtering were 1 Å s^{-1} and 5×10^{-3} mbar, respectively. The substrates were rotated at a speed of about 30 rotations per minute (rpm) during sputtering in order to ensure uniformity of a deposited metal film.

Pt/Anodisc™ was used as a working electrode for electrodeposition. Aqueous solution was prepared containing freshly distilled pyrrole monomer (25 mM) and $LiClO_4$ (100 mM) as a supporting electrolyte. Prior to electropolymerization, solution was deaerated by bubbling nitrogen gas for 10 min. Electropolymerization was carried out potentiostatically at 1.8 V applied potential. Optimization of thicknesses of Pt and PPy nanotubes is of utmost importance in order to obtain the nanoporous electrode as shown in Fig. 1, for the improved performance

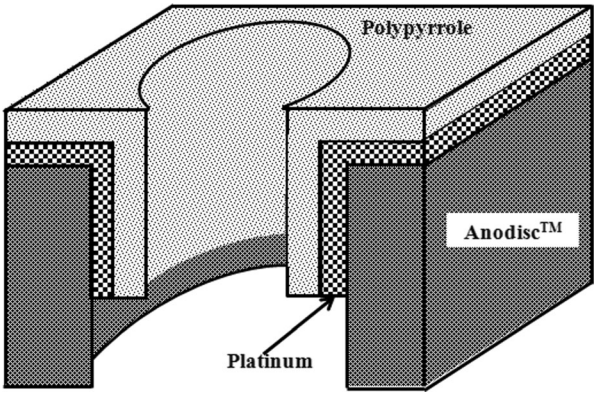

Fig. 1 Schematic illustration of a cross-sectional view of polymerized electrode

of biosensor. Hence, Pt thickness was varied from 25 to 100 nm, and polymerization duration was varied from 10 to 100 s for different samples. The surface morphologies of the produced Pt and PPy films were investigated using field emission scanning electron microscope (FESEM, Carl Zeiss SUPRA55).

Also, porosity of Pt-coated electrode before and after polymerization for different durations was calculated using an image processing tool in Matlab by transforming the grayscale images obtained from FESEM into binary images (having only black and white regions, where black regions correspond to the regions containing pores on the electrode), and thus, a calculation based on the ratio of area occupied by black pixels to the total area of the image (black+white) led to the estimation of the porosity of the Pt/PPy-modified Anodisc-based electrodes.

4. Enzyme immobilization and quantification

Immobilization refers to the attachment of enzymes to a solid surface so as to confine their movement. In the view of preventing enzymes from denaturing, physical adsorption was chosen as the suitable method [6]. GO_x solution (10 mg ml^{-1}) was prepared in 50 mM PBS (pH 6.8). Enzyme immobilization was carried out by physical adsorption of 10 μl aliquot from GO_x solution placed onto polymerized surface (PPy/Pt/Anodisc™), and electrode was allowed to dry in an incubator at 4 °C. Subsequently, electrode was washed thoroughly in PBS to remove loosely adhered enzyme molecules away from the sensing electrode, dried, and stored at 4 °C when not being used.

Each GO_x molecule contains aromatic residue called tryptophan, which contributes to the intrinsic fluorescence in this molecule. Tryptophan fluorescence can be excited at 295 nm, and its emission can be measured at 340 nm [23]. Since intensity of the fluorescence emission at 340 nm is directly proportional to the amount of enzyme used for the measurement. Therefore, this optical characteristic of GO_x was used for quantification of immobilized enzyme. Fluorescence emission spectra were obtained using FluoroMax-4p spectrofluorometer from Horiba Jobin Yvon (Model: FM-100). Excitation and emission slits were set at 2 nm each. Steady-state fluorescence was measured for known amounts of GO_x in PBS (50 mM), and a plot was obtained for intensity versus amount of GO_x, which followed a linear relationship and served as a calibration plot for enzyme quantification. As a known amount of GO_x (100 μg) was used for enzyme immobilization, PBS containing unadhered GO_x molecules obtained by thorough washing of electrodes was collected separately for each sensing electrode, followed by

fluorescence measurement. Amount of unadhered GO_x molecules was estimated by comparing the intensity values with calibration plot. Subtraction of the corresponding amount from 100 μg (total amount of enzyme used for immobilization) led to an estimate of loaded enzyme for each of the sensing electrodes.

5. Amperometric detection of glucose

Equations (1), (2), and (3) represent the basic principle of the amperometric enzymatic glucose biosensing. As also shown in Fig. 2, GO_x immobilized on supporting matrix catalyzes oxidation of glucose ($C_6H_{12}O_6$) into gluconic acid ($C_6H_{12}O_7$). Hydrogen peroxide (H_2O_2), a byproduct of this reaction, decomposes into electrons and ions due to an applied potential of 0.7 V at anode [4, 24]. Therefore, current proportional to the glucose concentration flows in the circuit. Hence, the biosensor device can be calibrated in terms of the measured current.

$$C_6H_{12}O_6 + GO_x(ox) \rightarrow C_6H_{12}O_7 + GO_x(red) \quad (1)$$

$$GO_x(red) + O_2 + H_2O \rightarrow GO_x(ox) + H_2O_2 \quad (2)$$

$$H_2O_2 \xrightarrow{0.7\ V} 2H^+ + 2e^- + O_2 \quad (3)$$

Stock solution of 1 M glucose was prepared in DI water and allowed to mutarotate overnight before use in order to establish the equilibrium concentrations between α and β anomers [1]. GO_x solution (10 mg ml^{-1}) was prepared in 50 mM PBS. Glucose biosensing response was examined using amperometric detection technique. Sensing electrode (GO_x/PPy/Pt/Anodisc™) was used as working electrode in a three-electrode electrochemical cell. The electrodes were all immersed in PBS (50 mM, pH 6.8), and solution was constantly stirred mechanically at 200 rpm in order to provide convective transport to analyte (glucose) molecules. A fixed potential of 0.7 V was applied to the working electrode, and background current was allowed to decay to a steady state before aliquots of glucose solution were added into the cell. Increments in current density upon successive additions of glucose (≥5 μl) were recorded against time.

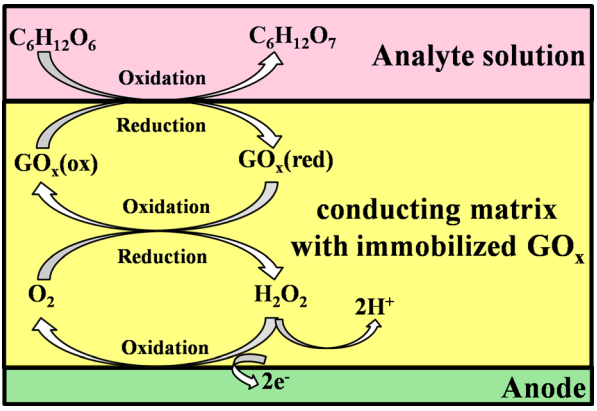

Fig. 2 Schematic of enzyme-catalyzed glucose oxidation on surface of a transducer

Important biosensor characteristics, viz., sensitivity, response time, lower detection limit, and linear range of operation, were estimated for the fabricated biosensors.

Results and Discussion

1. Enzyme activity assay

Enzymes being very much sensitive to the environmental conditions, viz., temperature, pH, etc., are required to determine the specific activity of enzymes prior to their usage for immobilization purposes. Specific activity is defined as micro-moles of substrate converted into product per minute by enzyme contained in 1 mg of protein [25]. The conventional colorimetric assays require coupling of H_2O_2 (produced by glucose oxidation) with some other chemical compound or dye in the presence of a second enzyme (horseradish peroxidase) in order to facilitate absorption in the visible region for activity assay. The environmental and chemical sensitivity of these chemical reagents and dependence of measurement on the activity of the second enzyme may often lead to inconsistent results.

Hence, specific activity of GO_x was determined using much simpler and straight forward electrochemical assay [26]. From Eqs. (1), (2), and (3), it is evident that concentration of H_2O_2 is directly related with the concentration of glucose present in the sample. Hence, known concentrations of H_2O_2 (1–500 μM) in 50 mM PBS (pH 6.8) were readily used. For each concentration, steady-state current was obtained in a three-electrode electrochemical cell for the voltage 0.7 V applied to Pt-working electrode vs. reference electrode under constant stirring (200 rpm). Figure 3 shows H_2O_2 calibration curve plotted between steady-state current and H_2O_2 concentration. It follows linear relationship with slope $\partial I/\partial[H_2O_2]=0.24$ A M^{-1}, indicating that change in current is correlated with change in H_2O_2 concentration. Therefore, rate of change of current can also be correlated with the rate of change of H_2O_2 concentration.

For activity assay, known concentrations of glucose solution prepared in 50 mM PBS were used in an electrochemical cell. Again, 0.7 V potential was applied to a working electrode. After achieving a steady-state current, 20 μl (200 μg) GO_x from stock solution (10 mg ml^{-1} in

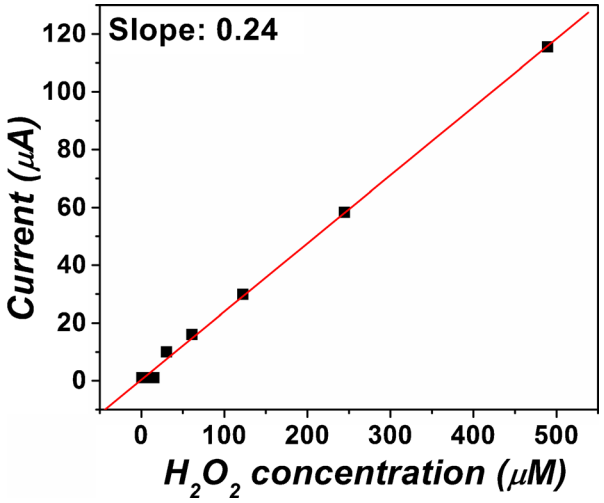

Fig. 3 H_2O_2 calibration curve (1–500 μM range)

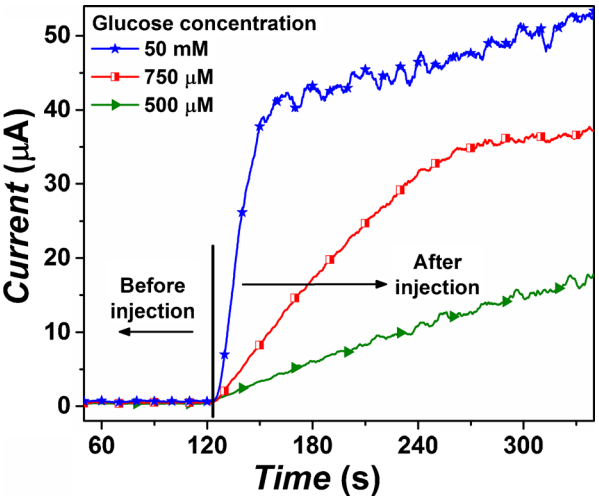

Fig. 4 GO_x assay curve for glucose concentration 500, 750, and 50 mM

50 mM PBS) was injected. Instantaneous rise in current was observed as shown in the chronoamperometric curves in Fig. 4. The experiment was repeated for higher glucose concentrations starting from a minimum of 50 μM. The maximum slope of current $(\partial I/\partial t)_{max}$=4.43 μA s^{-1} observed for 50 mM glucose concentration corresponds to the highest attainable reaction rate. No increase in slope was observed for glucose concentrations higher than 50 mM, indicating that all of the active sites of enzyme were occupied by the substrate molecules at this concentration. Therefore, enzymatic glucose oxidation reaction was no more dependent on substrate concentration. Thus, specifie activity (A) was calculated according to Eq. (4).

$$A = \left((\partial I/\partial t)_{max} / \partial I/\partial [H_2O_2] \right) \times \left(\frac{5 \times 60}{50} \right) \tag{4}$$

A multiplication factor of $\frac{5\times60}{50} = 6$ (5 to convert 200 μg GO_x into 1 mg, 1/50 to convert H_2O_2 molar concentration into number of H_2O_2 molecules in a 20-ml solution volume, and 60 to convert time from seconds to minutes) was introduced in order to obtain the specific activity in desired unit (μm min^{-1} mg^{-1}). Thus, specific activity was computed as 111 U mg^{-1} (1 U= 1 μm substrate conversion min^{-1}).

2. Amperometric measurements on biosensor

Glucose biosensing response was examined for the biosensors obtained for different polymerization durations (10–100 s). Figure 5 shows the amperometric response curve for the biosensor with polymerization time of 40 s. Similar response curves were also obtained for remaining biosensors also (not shown here). Current response represents the rate of oxidation of glucose by the GO_x immobilized in the PPy matrix. Inset in Fig. 5 clearly shows a step-like response observed for each successive addition of glucose. This is a clear indication for retention of GO_x activity upon immobilization and strong affinity of substrate with an enzyme. Therefore, current increases sharply and attains steady state upon injection of glucose. Estimated response time was observed lying typically in the range of 10–15 s for all

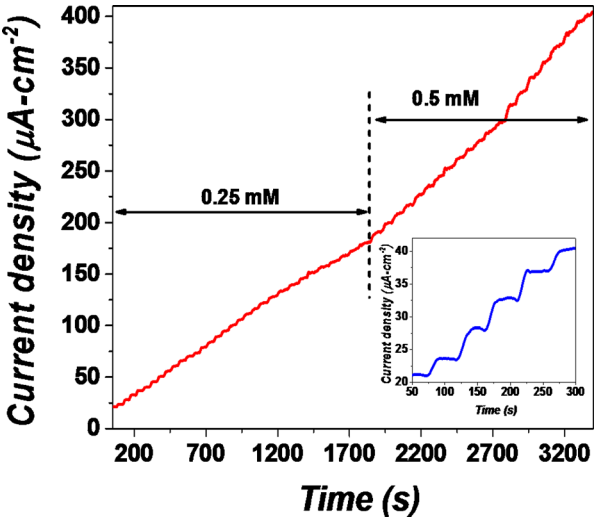

Fig. 5 Amperometric response curve for the biosensor with polymerization time 40 s

biosensors. For each biosensor, calibration curve was further derived from an amperometric response curve, which relates steady-state current density with glucose concentration. Calibration curves for the biosensors with polymerization times 30, 40, 50, and 100 s are shown in Fig. 6. As evident from these curves, current density rises linearly for lower concentrations and tends to saturate at higher concentrations. This behavior dictates the enzyme kinetics. As also observed in activity assay, at higher concentrations, occupancy of all active sites of enzymes by glucose molecules leads to saturated response [27]. Therefore, linear range of biosensor was estimated by linear regression analysis of the plotted calibration curve.

Further, it should be noted that the sensitivity was estimated from the slope of the calibration curve for each of the fabricated biosensor. Figure 7 shows the sensitivity values obtained for all biosensors. The highest sensitivity of 18.6 mA cm^{-2} M^{-1}, over a wide linear range of operation (0.25–20 mM), and the lowest detection limit of 0.25 mM were obtained for

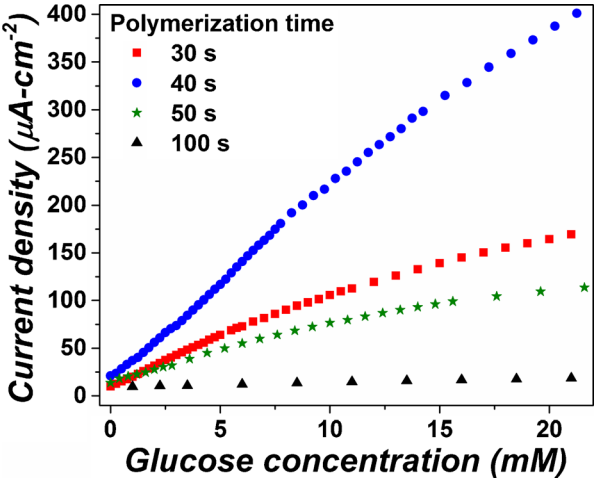

Fig. 6 Calibration curves for biosensors with polymerization time 30, 40, 50, and 100 s

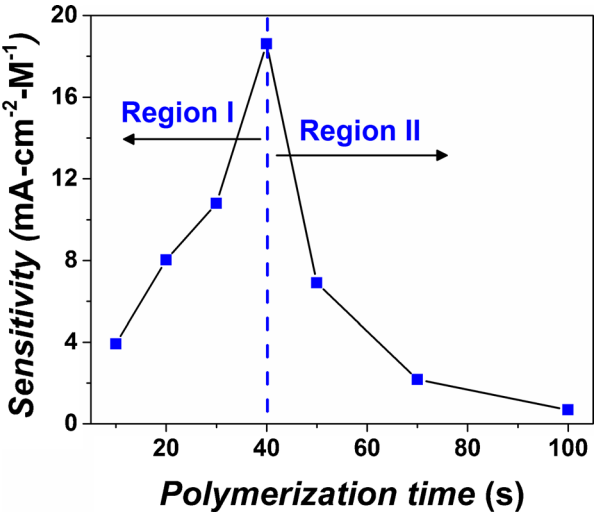

Fig. 7 Sensitivity values for biosensors with polymerization time from 10 to 100 s

polymerization time of 40 s. In this figure, regions I and II correspond to polymerization time <40 s and >40 s, respectively. Further, the sensitivity values were found to decrease sharply for both, increased as well as decreased polymerization durations. However, the reasons for the apparent degraded performances may be different for regions I and II (as can be seen in Fig. 7) and needs further investigation.

3. Characterization of electrode surfaces

To investigate the strong influence of polymerization time on the biosensor sensitivity and the reason for the observed, optimized behavior of biosensor for polymerization duration of 40 s, surface morphologies of the Pt electrode, and grown PPy films were studied using FESEM. In order to make the surface and porous walls of alumina template sufficiently conducting along with preserving the porous nanostructure for subsequent polymerization, immobilization, and biosensing; thickness of Pt coated on Anodisc™ was varied from 25 to 100 nm. A thickness of 50 nm was found to be optimum in this regard. A similar fact was observed by Ekanayake et al. [15] also. Figure 8a shows a top view SEM image of Anodisc™ after 50-nm thick Pt deposition. As can be seen, the surface was covered with the spherical nanoparticles of size less than 40 nm. Figure 8b–e show SEM images of the polymerized electrodes for the polymerization durations 30, 40, 50, and 70 s, respectively. In order to estimate the length of nanotubes, sample was prepared separately. After polymerization, Anodisc™ was dissolved carefully by immersing it in 1 M NaOH solution for 2 h, washed thoroughly with DI water many times, and dried under a vacuum [28]. Figure 8f shows the cross-sectional view of the nanotubes. The obtained length of the nanotubes was approximately 1.5 μm.

Porosity of Anodisc™ after Pt deposition was calculated to be approximately 26 %. Figure 9 shows calculated porosity values and amount of loaded enzyme per unit area of electrode corresponding to polymerization for different times (10–100 s). Regions I and II have similar definitions as in Fig. 7. As polymerization was carried out successively for higher time durations, porosity of electrode decreased due to PPy deposition inside the pores. Electrode retained 18.6 % porosity for polymerization time of 40 s, after which significant drop in

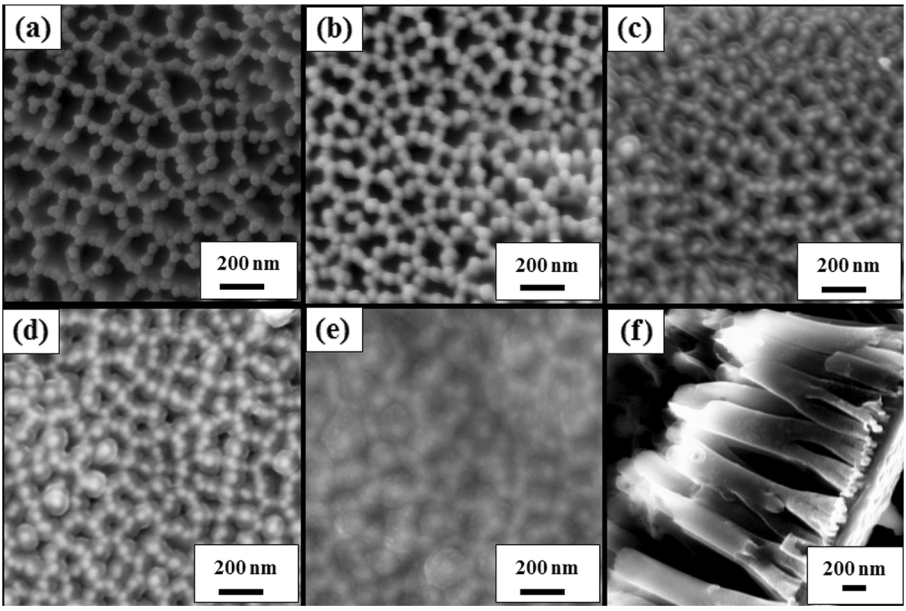

Fig. 8 FESEM top view images of **a** 50 nm Pt-coated Anodisc™, polymerized electrode for **b** 30, **c** 40, **d** 50, and **e** 70 s time and **f** cross-sectional view of Pt nanotubes

porosity was recorded. Eventually, for 100 s polymerization time, pores were almost completely blocked by the deposited PPy film, resulting in no porous structure at all.

The strong dependence of sensitivity on the polymerization time was attributed to the mechanism of nucleation and growth of PPy on the surface and porous walls of the electrode. According to the progressive nucleation and growth model, in the early stages of potentiostatic electropolymerization, PPy nodules nucleate and grow three dimensionally [29, 30]. As polymerization continues, the smaller nodules grow further and later join to form larger polymer aggregates. The obtained SEM images in Fig. 8 are in accordance with this growth

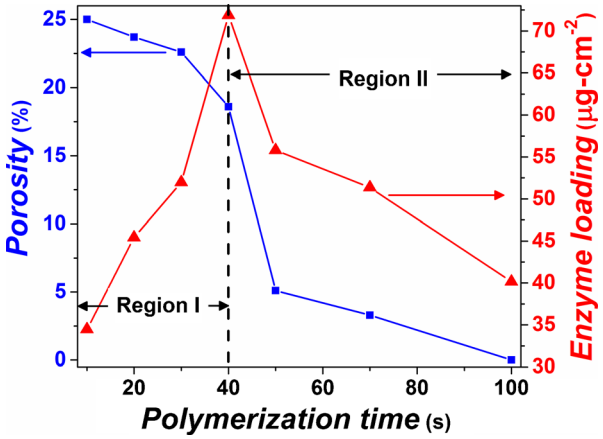

Fig. 9 Calculated values of porosity and amount of enzyme loaded per unit area of electrode for different polymerization times (10–100 s)

pattern. For smaller polymerization times (up to 30 s), due to small size of polymer nodules, the surface area of PPy available for enzyme loading is limited. As polymerization time was increased from 10 to 30 s, increased surface area of nodules led to increase in sensitivity from 3.9 mA cm^{-2} M^{-1} (for 10 s) to 10.8 mA cm^{-2} M^{-1} (for 30 s). However, the polymerization time of 40 s is optimum for formation of aggregates with the full coverage of the Pt surface. Hence, maximum surface area along with sufficiently opened pores maximizes GO_x loading during immobilization process (Figs. 8c and 9). As sensitivity highly depends upon the amount of immobilized enzyme, it showed a sharp increase to a value of 18.6 mA cm^{-2} M^{-1} for this biosensor. The thickness of grown PPy is proportional to the total amount of the charge associated with pyrrole oxidation per unit area of electrode. Table 1 lists the charge density along with the sensitivity values associated with biosensors for all seven polymerization times.

If the electrooxidation is carried out for higher time durations (>40 s), due to the growth of thicker PPy films, the inner walls of polymer-coated nanotubes approach closer. This in turn decreases the surface area and shrinks the pores thereby obstructing the enzyme loading and passage of analyte molecules up to some extent (Figs. 8 and 9). At 50 s polymerization time (Fig. 8d), sensitivity reduced to a value 6.9 mA cm^{-2} M^{-1}, which is less than half of the maximum sensitivity. The clogging of pores was further pronounced for higher polymerization times, affecting the observed sensitivity severely. The lowest sensitivity of 0.7 mA cm^{-2} M^{-1} was obtained for a polymerization time of 100 s, for which the pores were almost completely blocked by the grown PPy film (SEM image not shown).

A careful analysis of the observed trend in the sensitivity, enzyme loading, and porosity suggests that the sensitivity of the fabricated biosensors depended upon two factors: [1] amount of GO_x immobilized on PPy-covered Pt electrode surface and [2] porosity of the PPy electrode. In region I, porosity of electrodes is reasonably good, but polymerization time (<40 s) was too short for sufficient growth of PPy nodules. Hence, incomplete coverage of Pt electrode by PPy restrains the extent of enzyme loading. In region II, though polymerization time (>40 s) is sufficient for complete coverage of Pt surface, however, once Pt electrode surface is completely covered by PPy (corresponding to polymerization time 40 s), for higher polymerization times (>40 s), growth of thicker PPy film leads to narrowing of the pore diameter of the resultant electrode, which in turn reduces the PPy surface area available for enzyme immobilization. Thus, in region II, restriction on sensitivity of biosensor was imposed by substantial narrowing of nanopores due to higher thicknesses of grown PPy in this

Table 1 Details of charge density associated with polymerization and sensitivity of the biosensors

Polymerization time (s)	Charge density (mC cm^{-2})	Sensitivity (mA cm^{-2} M^{-1})
10	57.1	3.9
20	176.1	8.0
30	239.2	10.8
40	287.1	18.6
50	401.9	6.9
70	778.4	2.2
100	1,260.0	0.7

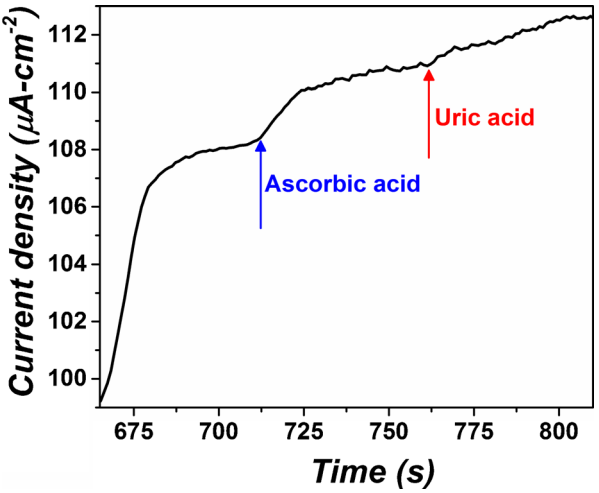

Fig. 10 Influence of electroactive interferents (uric acid, ascorbic acid) on biosensor response

region, which hampered overall enzyme immobilization. An adequate balance between the Pt surface coverage by PPy and electrode porosity for the optimized polymerization time of 40 s led to highest sensitivity for this biosensor, as was also verified by FESEM images of these electrodes, their respective porosity calculations, and estimated enzyme loading.

Influence of electroactive interferents: uric acid (0.1 mM) and ascorbic acid (0.1 mM) on biosensing response of the optimized biosensor was examined in the presence of 5.5 mM glucose in PBS [31]. As shown in Fig. 10, a small increase of 4.8 % in response current density was observed. This establishes suitability of this biosensor in diagnosis of real blood samples.

Table 2 presents a comparison of important biosensor characteristics of the biosensor developed in this study with biosensors reported recently by various groups, in which similar PPy nanostructures were utilized as an immobilization matrix [15, 17, 32–34]. Thus, the developed biosensor demonstrated higher sensitivity and extended linear range of operation with reasonable response time.

Table 2 Comparison of present work with recently reported similar glucose biosensors

S. No.	Sensing matrix	Sensitivity (mA cm^{-2} M^{-1})	Linear range (mM)	Response time (s)	Reference
1	AAO/Pt/PPy/GO_x nanotube arrays	18.6	0.25–20	10	This work
2	AAO/Pt/PPy/GO_x nanotube arrays	7.4	0.5–13	3	[15]
3	AAO/Au/GO_x/PPy	0.08	0–5	15	[32]
4	PPy/GO_x nanowire arrays	9.97	0.1–8	7	[33]
5	PPy/GO_x/SWCNTs-$PhSO_3^-$	6	0.02–6	–	[17]
6	Alginate-PPy matrix	16	0–3.5	4	[34]

Conclusions

It has been demonstrated that the nanoporosity of grown PPy nanotubes plays a very crucial role in immobilization and subsequent biosensing. The extended range of linear operation of biosensing device for the optimized polymerization time of 40 s enables this device to be utilized for monitoring not only of diabetes but also in food industry where it is required to detect high glucose concentrations as well. The sensitivity, linear range of operation, and response time can further be improved by employing other immobilization techniques such as cross-linking, co-entrapment, etc.

Acknowledgments One of the authors P. A. P. is grateful to FESEM, Fluorescence and Potentiostat/Galvanostat facilities equipped at the Sophisticated Instrument Centre, IIT Indore. P. A. P. would also like to thank Dr. Mukul Gupta (University Grants Commission Department of Atomic Energy (UGC DAE) Consortium for Scientific Research Indore (M. P.), India) for the usage of the DC magnetron sputtering system. P. A. P. would further like to thank the Ministry of Human Resource and Development (MHRD), India for providing the Teaching Assistantship (TA). Author V. S. would like to thank director of IIT Indore for providing the seed grant for the research.

References

1. Vasudevan, D. M., & Sreekumari, S. (2005). In J. Brothers (Ed.), *Textbook of biochemistry for medical students*. Medical Publishers: New Delhi.
2. MacLeod, A. J. (1973) Instrumental methods of food analysis. ed. Elek Science, London.
3. Newman, J. D., & Turner, A. P. F. (2005). Home blood glucose biosensors: a commercial perspective. *Biosensors and Bioelectronics, 20*, 2435–2453.
4. Wang, J. (2008). Electrochemical glucose biosensors. *Chemical Reviews, 108*, 814–825.
5. Prodromidis, M. I., & Karayannis, M. I. (2002). Enzyme based amperometric biosensors for food analysis. *Electroanalysis, 14*, 241–261.
6. Sheldon, R. A. (2007). Enzyme immobilization: the quest for optimum performance. *Advanced Synthesis & Catalysis, 349*, 1289–1307.
7. Guimard, N. K., Gomez, N., & Schmidt, C. E. (2007). Conducting polymers in biomedical engineering. *Progress in Polymer Science, 32*, 876–921.
8. Rajesh, P. S. S., Takashima, W., & Kaneto, K. (2004). Development of an amperometric biosensor based on a redox-mediator-doped polypyrrole film. *Journal of Applied Polymer Science, 93*, 927–933.
9. Vidal, J.-C., Garcia-Ruiz, E., & Castillo, J.-R. (2003). Recent Advances in electropolymerized conducting polymers in amperometric biosensors. *Microchimica Acta, 143*, 93–111.
10. Gurunathan, K., Murugan, A. V., Marimuthu, R., Mulik, U. P., & Amalnerkar, D. P. (1999). Electrochemically synthesised conducting polymeric materials for applications towards technology in electronics, optoelectronics and energy storage devices. *Materials Chemistry and Physics, 61*, 173–191.
11. Cosnier, S. and Karyakin, A. (2010) Electropolymerization: concepts, materials and applications. ed. Wiley-VCH Verlag GmbH & Co. KGaA Germany.
12. Wallace, G. G., Tsekouras, G. and Wang, C. (2010), in Electropolymerization, Wiley-VCH Verlag GmbH & Co. KGaA, pp. 215-240.
13. Huang, J., Wang, K., & Wei, Z. (2010). Conducting polymer nanowire arrays with enhanced electrochemical performance. *Journal of Materials Chemistry, 20*, 1117–1121.
14. Li, C., Bai, H., & Shi, G. (2009). Conducting polymer nanomaterials: electrosynthesis and applications. *Chemical Society Reviews, 38*, 2397–2409.
15. Ekanayake, E. M. I. M., Preethichandra, D. M. G., & Kaneto, K. (2007). Polypyrrole nanotube array sensor for enhanced adsorption of glucose oxidase in glucose biosensors. *Biosensors and Bioelectronics, 23*, 107–113.
16. Ekanayake, E. M. I., Preethichandra, D. M. G., & Kaneto, K. (2008). Effect of glucose oxidase immobilizing techniques on performances of nano scale polypyrrole glucose biosensors. *Japanese Journal of Applied Physics, 47*, 1321–1324.

17. Raicopol, M., Pruna, A., Damian, C., & Pilan, L. (2013). Functionalized single-walled carbon nanotubes/polypyrrole composites for amperometric glucose biosensors. *Nanoscale Research Letters, 8*, 316–323.
18. Ramanavičius, A., Ramanavičienė, A., & Malinauskas, A. (2006). Electrochemical sensors based on conducting polymer—polypyrrole. *Electrochimica Acta, 51*, 6025–6037.
19. Debiemme-Chouvy, C. (2009). Template-free one-step electrochemical formation of polypyrrole nanowire array. *Electrochemistry Communications, 11*, 298–301.
20. Martin, C. R. (1995). Template synthesis of electronically conductive polymer nanostructures. *Accounts of Chemical Research, 28*, 61–68.
21. Chakarvarti, S. K., & Vetter, J. (1998). Template synthesis—a membrane based technology for generation of nano-/micro materials: a review. *Radiation Measurements, 29*, 149–159.
22. Xiao, R., Cho, S. I., Liu, R., & Lee, S. B. (2007). Controlled electrochemical synthesis of conductive polymer nanotube structures. *Journal of the American Chemical Society, 129*, 4483–4489.
23. Small, E. W. (1991). in Topics in fluorescence spectroscopy. ed. Plenum, New York.
24. Clark, L. C., & Lyons, C. (1962). Electrode systems for continuous monitoring in cardiovascular surgery. *Annals of the New York Academy of Sciences, 102*, 29–45.
25. Wilson, K. and Walker, J. M. (2005) Principles and techniques of biochemistry and molecular biology. ed. Cambridge University Press, United Kingdom.
26. Wrolstad, R. (2001). Current protocols in food analytical chemistry. ed. Wiley, New York.
27. Holland, J. T., Harper, J. C., Dolan, P. L., Manginell, M. M., Arango, D. C., Rawlings, J. A., Apblett, C. A., & Brozik, S. M. (2012). Rational redesign of glucose oxidase for improved catalytic function and stability. *PloS One, 7*, e37924.
28. Kotz, J. C. and Purcell, K. F. (1987). Chemistry & chemical reactivity ed. Saunders College Pub., Philadelphia.
29. Heinze, J., Frontana-Uribe, B. A., & Ludwigs, S. (2010). Electrochemistry of conducting polymers—persistent models and new concepts. *Chemical Reviews, 110*, 4724–4771.
30. Hernández-Pérez, T., Morales, M., Batina, N., & Salmón, M. (2001). Effect of the electrosynthesis method on the surface morphology of the polypyrrole film—an atomic force microscopy study. *Journal of The Electrochemical Society, 148*, C369–C375.
31. Zhao, K., Zhuang, S., Chang, Z., Songm, H., Dai, L., He, P., & Fang, Y. (2007). Amperometric glucose biosensor based on platinum nanoparticles combined aligned carbon nanotubes electrode. *Electroanalysis, 19*, 1069–1074.
32. Liu, L., Jia, N., Zhou, Q., & Jiang, Z. (2007). Electrochemically fabricated nanoelectrode ensembles for glucose biosensors. *Materials Science and Engineering C, 27*, 57–60.
33. Xu, G. Q., Lv, J., Zheng, Z. X. and Wu, Y. C. (2012). Polypyrrole (PPy) nanowire arrays entrapped with glucose oxidase biosensor for glucose detection. *Nano/Micro Engineered and Molecular Systems (NEMS), 2012 7th IEEE International Conference on*, pp. 511-514.
34. Rabeah, K. A., & Marks, R. S. (2009). Impedance study of the hybrid molecule alginate-pyrrole: demonstration as host matrix for the construction of a highly sensitive amperometric glucose biosensor. *Sensors and Actuators B, 136*, 516–522.